Available online at www.sciencedirect.com
SCIENCE DIRECT
Journal of Catalysis 233 (2005) 136–146
JOURNAL OF CATALYSIS
www.elsevier.com/locate/jcat

Selective oxidation of benzene to phenol with nitrous oxide over MFI zeolites. 2. On the effect of the iron and aluminum content and the preparation route

E.J.M. Hensen *, Q. Zhu, R.A. van Santen

Schuit Institute of Catalysis, Laboratory of Inorganic Chemistry and Catalysis, Eindhoven University of Technology, P.O. Box 513, 5600 MB, Eindhoven, The Netherlands

Received 12 October 2004; revised 19 March 2005; accepted 8 April 2005

Available online 23 May 2005

Abstract

Iron- and/or aluminum-containing MFI zeolites were prepared via various routes, including isomorphous substitution followed by thermal activation and grafting reactions with molecular Fe or Al precursors over [Al]MFI and [Fe]MFI, respectively. The effect of the iron and aluminum content on the performance in benzene oxidation with nitrous oxide at 623 K was studied for a suite of isomorphously substituted zeolites. The activity increased with increasing iron and aluminum content. Steamed zeolites were more active than their calcined counterparts. The extent of coking deactivation increased with initial activity and tallies with a consecutive reaction mechanism in which phenol further reacts to products that cannot leave the zeolite micropores. A very small amount of iron is involved in the selective oxidation reaction. A strong correlation is observed between the initial rate of phenol formation and the intensity of the infrared band at 1635 cm^{-1} due to NO_2 interacting with extraframework Fe–O–Al. On the other hand, nitrous oxide decomposition at higher temperatures is suggested to be mainly catalyzed by more clustered Fe species. Alternative preparation routes that use grafting of trimethylaluminum or iron chloride on otherwise inactive ferrosilicalite and aluminosilicalite, respectively, provide further support for the necessity of extraframework mixed iron–aluminum-oxo species. Steaming at high temperature is not only important for removal of the catalytically active metals from the zeolite framework, but also improves the formation of active sites. A case in point is the dispersion of Fe and Al in the micropores of silicalite-1, which renders an active, selective, and stable catalyst.
© 2005 Elsevier Inc. All rights reserved.

Keywords: Iron; Aluminum; Zeolite; MFI; Selective oxidation; Benzene; Phenol; Nitrous oxide; Active sites; Trimethylaluminum; Sublimation

1. Introduction

Selective oxidation of organic materials into more valuable chemicals remains one of the largest challenges in catalytic chemistry [1]. In the last two decades, a considerable effort has been made to understanding ZSM-5-based catalysts for the selective oxidation of benzene to phenol by nitrous oxide [2–48]. In particular, the location and structure of iron species active in the title reaction and among others in nitrous oxide decomposition and NO_x reduction have been widely addressed. These appear to depend strongly on the preparation method and the mode of pretreatment [5–48]. The debate concerning the selective oxidation of benzene with nitrous oxide concentrates on the constitution of the active sites. In a companion contribution [48], we gave an overview of the various proposals concerning the active sites. Despite the propensity of such proposals, it is fair to say that there is currently some consensus on the role of extraframework Fe species as the main component for the active sites [8,10,18,21,23,38,41–48], showing a specific redox behavior, with nitrous oxide as oxidant [10]. Nitrous oxide

* Corresponding author. Fax: +31 40 2455054.
E-mail address: e.j.m.hensen@tue.nl (E.J.M. Hensen).

0021-9517/$ – see front matter © 2005 Elsevier Inc. All rights reserved.
doi:10.1016/j.jcat.2005.04.008

may decompose to molecular nitrogen and leave an oxygen atom on the catalytic surface, via $N_2O + [\ ] \rightarrow N_2 + [O]$, where [ ] and [O] refer to the empty Fe^{2+} vacancy and an active oxygen species deposited on Fe^{3+}, respectively. The nature of the deposited oxygen atom is not clear, however. It may be selectively inserted into C–H bonds of alkanes and aromatics.

The nature and further composition of the active sites remain points of intense debate. Although the sole role of Al species as the active sites [2–4] was challenged by several authors [8,9,38], we have provided evidence [44,47,48] for the necessity of Al in active catalysts. Another important issue relates to the location of the Al species constituent of these active sites. Whereas the active sites are usually supposed to be made up of positively charged iron oxo species of low nuclearity coordinating to the negatively charged aluminum-occupied oxygen tetrahedra of the zeolite, we have proposed that ferrous ions stabilized on extraframework Al species are the active species [44,46–48]. This contribution primarily seeks to provide further support for the hypothesis that extraframework mixed iron–aluminum oxide species are active in the decomposition of nitrous oxide and the subsequent hydroxylation of benzene to phenol. To this end, we have prepared iron- and/or aluminum-containing zeolites via different routes encompassing isomorphous substitution of the metals in the MFI lattice by hydrothermal synthesis followed by steam activation, grafting of molecular iron and aluminum species on alumino- and ferrosilicalite, respectively, and the postsynthesis dispersion of iron and aluminum oxides in silicalite-1.

We have prepared a larger set of isomorphously substituted MFI zeolites of different compositions in a parallel batch autoclave. This provides insight into the effect of the Fe and Al contents, which has been addressed only occasionally before. Kubanek et al. [38] compared various zeolites with iron contents in the range of 0.03–0.2 wt% (the zeolite, however, mostly having different Al contents) and found that the activity is linked to cationic iron species. Nevertheless, a positive correlation between the activity and the amount of extraframework Al species was noted. Meloni et al. [21] noted that the deactivation rate correlated with the total surface acidity. Berlier et al. [22] performed a detailed NO IR study on a wide range of MFI zeolites containing different levels of Fe and/or Al. Their conclusions describe the active sites in terms of isolated Fe^{2+} centers in proximity to (framework) Al, thus challenging the proposition of binuclear Fe clusters. Yuranov et al. [41] related benzene hydroxylation activity to mono- and oligonuclear Fe sites with the use of zeolites with different Fe and Al loadings. Kinetics for benzene oxidation were studied in detail by Ivanov et al. [49].

In the present study, we will mainly employ benzene oxidation with nitrous oxide to study the activity of the various zeolites. In some cases, we will compare this with temperature-programmed nitrous oxide decomposition. These data will be complemented by infrared spectroscopy characterization.

2. Experimental

2.1. Catalyst preparation

Zeolites with the MFI topology and with various Fe and Al contents were prepared by hydrothermal synthesis in a parallel batch autoclave. This autoclave permits the simultaneous hydrothermal synthesis of nine zeolites of different composition. To this end, 102.4 g tetraethylorthosilicate (TEOS) (Acros; 98%) was added to 150 g organic template tetrapropylammonium hydroxide (TPAOH) (Fluka; 20% in water) and vigorously stirred overnight. Portions of this solution were added to appropriate amounts of solutions containing iron nitrate ($Fe(NO_3)_3{\cdot}9H_2O$, 98%; Merck) and/or aluminium nitrate ($Al(NO_3)_3{\cdot}9H_2O$, 99%; Janssen) of different concentration(s) with vigorous stirring. The nine mixtures were then transferred into small cylinders made of PEEK, each with a volume of 30 ml. Sealing was achieved with Kalrez rings in the PEEK lids. These cylinders were then placed in a larger stainless-steel vessel covered by a stainless-steel lid. The autoclave was kept at 443 K for 5 days. After filtration, washing, and drying at 383 K overnight, white zeolite powders were obtained in all cases.

The successful synthesis of zeolites with the MFI topology was confirmed by X-ray diffraction. Subsequently, the organic template was carefully removed by the following calcination procedure: (i) zeolite was treated in 100 ml min^{-1} N_2 during heating to 823 K at a ramp rate of 1 K min^{-1} and kept at this temperature for 8 h. (ii) The material was further treated in 100 ml min^{-1} 20 vol% O_2 in N_2 at 823 K for another 4 h. Steam activation was achieved by heating of the catalyst in a flow of 20 vol% oxygen in N_2 to 973 K at a rate of 1 K min^{-1}, followed by exposure to a mixture of 10 vol% H_2O and 18 vol% O_2 in N_2 for 3 h. The calcined zeolites are denoted as [Fe,Al]MFI(x, y, [st]), where x stands for the weight percentage of iron and y for the Si/Al ratio. The materials modified by steaming are designated by (st). [Fe]MFI and [Al]MFI refer to the catalysts that have undergone substitution with only one hetero-atom.

Iron-silicalite ([Fe]MFI) was used as a precursor to incorporate Al via the deposition of trimethylaluminum. To this end, dehydrated [Fe]MFI, either calcined or steamed, was mixed with an excess of pure trimethylaluminum (Me_3Al; Aldrich) in an argon-flushed glove box. The methyl groups of Me_3Al are reactive toward hydroxyl groups. After 24 h, excess Me_3Al was removed by evacuation, and the sample was calcined at 823 K for 4 h. Some samples were further modified with a steaming treatment at 973 K. The resulting materials are denoted as [Fe]MFI + Me_3Al, [Fe]MFI(st) + Me_3Al, [Fe]MFI + Me_3Al(st), and [Fe]MFI(st) + Me_3Al(st). Incorporation of Fe into [Al]MFI was carried out by a sublimation method that was described extensively in our previous reports [45,46]. These catalysts are designated by the suffix "+$FeCl_3$."

Elemental analysis was carried out by ICP-OES, as described in a companion contribution [48]; the elemental

Table 1
Elemental composition of the zeolites as determined by ICP-OES

Catalyst	Al content (wt%)	Fe content (wt%)	Si/Al	Si/Fe
[Al]MFI	0.88	<0.001	42	–
[Fe]MFI	<0.005	0.55	–	143
[Fe,Al]MFI(0.0011,39)	0.96	0.0011	38	71,000
[Fe,Al]MFI(0.015,38)	0.96	0.015	38	5200
[Fe,Al]MFI(0.092,38)	0.96	0.092	38	850
[Fe,Al]MFI(0.45,42)	0.88	0.45	42	175
[Fe,Al]MFI(0.013,78)	0.48	0.013	78	6050
[Fe,Al]MFI(0.089,78)	0.48	0.089	78	880
[Fe,Al]MFI(0.46,77)	0.50	0.46	77	171
[Fe]MFI + Me_3Al	1.4	0.55	27	143
[Fe]MFI(st) + Me_3Al	1.4	0.55	27	143
[Al]MFI + $FeCl_3$	0.88	2.63	42	30
[Al]MFI(st) + $FeCl_3$	0.88	1.98	42	39
Si-1	<0.005	<0.001	–	–
Si-1 + Imp(Fe,Al)	0.98	0.61	37	129
Si-1 + Imp(Fe)	<0.005	0.62	–	129

compositions of the various materials are listed in Table 1.

2.2. Infrared spectroscopy

Infrared spectra of self-supporting catalyst wafers of approximately 12 mg were recorded at room temperature on a Bruker IFS-113v Fourier Transform IR spectrometer with a DTGS detector at a resolution of 2 cm^{-1}. Typically, a sample was pretreated in situ in oxygen at a temperature of 823 K for 1 h and cooled to room temperature in vacuo (pressure lower than 10^{-6} mbar). Subsequently, the sample was exposed to NO (purity >99.9%, 5 mbar) for 30 min at room temperature. Spectra were recorded after evacuation to study the region of adsorbed NO_2 species.

2.3. Activity measurements

Reaction data were collected in a single-pass atmospheric plug flow reactor. Analysis was performed by a well-calibrated combination of GC and MS. Before reaction, the catalyst was pretreated in a flow of 100 ml min^{-1} O_2/He (20 vol% O_2) during heating to 823 K at a rate of 1 K min^{-1}. We carried out benzene oxidation by feeding a mixture of C_6H_6/N_2O/He (volume ratio = 1:4:95) at a flow rate of 100 ml min^{-1} at a reaction temperature of 623 K. We used a feed of 0.5 vol% N_2O in He to test the activity in nitrous oxide decomposition. A more elaborate description of the activity measurements is available [48].

3. Results

3.1. Activity measurements

The rates of phenol formation for a suite of steam-activated zeolites with a Si/Al ratio of 40 with increasing Fe content as a function of reaction time are displayed in Fig. 1. The corresponding reaction parameters are condensed in Tables 2 and 3. [Al]MFI with residual Fe content showed negligible benzene and nitrous oxide conversion under the given reaction conditions. Introduction of a small amount of iron in [Fe,Al]MFI(0.0011,39,st) led to a significant increase in the rate of phenol formation. No deactivation with reaction time was observed, which is in line with the nearly quantitative conversion of benzene and nitrous oxide to phenol. A 14-fold increase in the iron content to 0.015 wt% brought about a threefold increase in the rate of phenol formation. This indicates that only a small portion of the iron atoms ended up in the active sites for benzene oxidation, even for zeolites with a very low iron content. This effect became more pronounced for a further increase in the iron content. A crude estimate of the initial turnover frequency (TOF) based on the assumption that in [Fe,Al]MFI(0.0011,39,st) all iron atoms are active gives a value of 0.4 s^{-1} under the given reaction conditions.

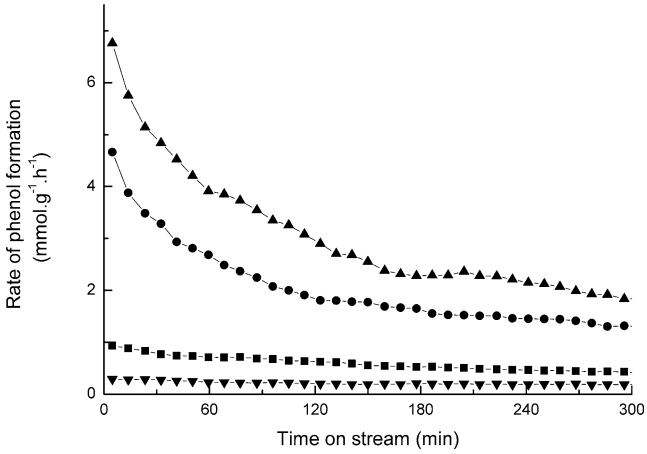

Fig. 1. Rate of phenol formation as a function of reaction time for (▼) [Fe,Al]MFI(0.0011,39,st), (■) [Fe,Al]MFI(0.015,38,st), (●) [Fe,Al]MFI(0.092,38,st), and (▲) [Fe,Al]MFI(0.45,42,st) (atmospheric pressure, reaction temperature 623 K, feed composition: 1 vol% benzene, 4 vol% N_2O, 95 vol% He, GHSV 30,000 h^{-1}).

The increase in iron content also resulted in decreased catalyst stability, as is evident from Fig. 1. The stronger deactivation of catalysts with higher initial activities coincides with lower initial selectivities of benzene and nitrous oxide to phenol. These selectivities were lowest for [Fe,Al]MFI(0.45,42,st). Side products of benzene oxidation included small amounts of carbon dioxide and water. However, the importance of full combustion was deemed to be minor because the selectivity for carbon oxides and water after a reaction time of 5 min was around 4% in [Fe,Al]MFI(0.45,42,st) and less than 1% in [Fe,Al]MFI(0.0011,39,st). These reaction products were no longer observed after a reaction time of 1 h for this set of catalysts. It is thus more likely that coke formation is the main side-reaction resulting in strong deactivation. This agrees well with earlier studies [21,49].

Fig. 2 compares the nitrous oxide conversion during its decomposition as a function of temperature for the steam-

Table 2
Initial phenol productivity (R_i), benzene conversion and selectivities to phenol and full combustion products during benzene oxidation for reaction times of 5 min, 1 h and 5 h

Catalyst	R_i [a]	Conversion (%)			Selectivity phenol (%)			Selectivity combustion (%)		
		5 min	1 h	5 h	5 min	1 h	5 h	5 min	1 h	5 h
[Al]MFI(st)	0.07	<1	–	–	–	–	–	–	–	–
[Fe,Al]MFI(0.0011,39,st)	0.29	1	1	1	>98	>98	>98	<1	<1	<1
[Fe,Al]MFI(0.015,38,st)	0.94	7	4	2	95	>98	>98	<1	<1	<1
[Fe,Al]MFI(0.092,38,st)	4.66	20	10	5	90	>98	>98	1	<1	<1
[Fe,Al]MFI(0.45,42,st)	6.76	32	14	6	80	>98	>98	3	<1	<1
[Fe,Al]MFI(0.45,42)	4.15	24	9	2	64	87	90	4	1.1	<1
[Fe,Al]MFI(0.013,78,st)	0.59	4	2	1	96	>98	>98	<1	<1	<1
[Fe,Al]MFI(0.089,78,st)	2.44	10	7	3	94	>98	>98	1	<1	<1
[Fe,Al]MFI(0.46,77,st)	5.45	29	14	7	73	96	>98	3	<1	<1
[Fe,Al]MFI(0.46,77)	3.35	15	9	5	84	90	90	3	<1	<1

Note: Reaction temperature 623 K, gas phase composition 1 vol% C_6H_6, 4 vol% N_2O, 95 vol% He, GHSV 30,000 h^{-1}).
[a] Phenol productivity (mmol g^{-1} h^{-1}) after a reaction time of 5 min.

Table 3
Nitrous oxide conversion and selectivity during benzene oxidation for reaction times of 5 min, 1 h and 5 h

Catalyst	Conversion (%)			Selectivity (%)		
	5 min	1 h	5 h	5 min	1 h	5 h
[Al]MFI(st)	<1	–	–	–	–	–
[Fe,Al]MFI(0.0011,39,st)	<1	<1	<1	>98	>98	>98
[Fe,Al]MFI(0.015,38,st)	2	1	<1	97	>98	>98
[Fe,Al]MFI(0.092,38,st)	6	2	1	73	>98	>98
[Fe,Al]MFI(0.45,42,st)	13	2	2	50	>98	>98
[Fe,Al]MFI(0.45,42)	9	3	<1	42	67	62
[Fe,Al]MFI(0.013,78,st)	1	<1	<1	>98	>98	>98
[Fe,Al]MFI(0.089,78,st)	3	2	1	84	>98	>98
[Fe,Al]MFI(0.46,77,st)	8	3	2	62	>98	>98
[Fe,Al]MFI(0.46,77)	7	3	1	50	59	51

Note: Reaction temperature 623 K, gas phase composition 1 vol% C_6H_6, 4 vol% N_2O, 95 vol% He, GHSV 30,000 h^{-1}.

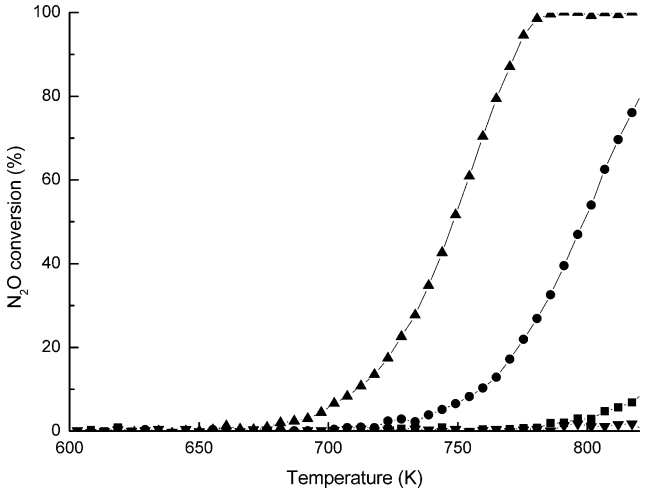

Fig. 2. Nitrous oxide conversion as a function of reaction time for (▼) [Fe,Al]MFI(0.0011,39,st), (■) [Fe,Al]MFI(0.015,38,st), (●) [Fe,Al]MFI(0.092,38,st), and (▲) [Fe,Al]MFI(0.45,42,st) (atmospheric pressure, feed composition: 0.5 vol% N_2O, make-up He, GHSV 30,000 h^{-1}).

activated materials with a Si/Al ratio close to 40. Again, one observes a strong increase in activity with iron content, although the activity differences appear to be substantially larger than they are during benzene oxidation. Close inspection of the reaction data shows that the intrinsic activity increased more than proportionally with iron content. For instance, an increase in the iron content from 0.092 to 0.45 wt% led to a tenfold increase in nitrous oxide conversion at 723 K. On the other hand, the nitrous oxide conversion for [Fe,Al]MFI(0.015,38,st) was only twice as high as it was for [Fe,Al]MFI(0.0011,39,st) at this temperature. This suggests that for catalytic nitrous oxide decomposition a different type of Fe species is active than for benzene oxidation. Another point worthy of note is the negligible nitrous oxide conversion at 623 K in catalytic nitrous oxide decomposition. This implies that benzene was oxidized by deposited oxygen atoms generated at the catalytic surface by the decomposition of nitrous oxide.

The activity and selectivity data (Fig. 3 and Tables 2 and 3) for the zeolites with a Si/Al ratio close to 80 followed a pattern very similar to the one for the zeolites with a Si/Al ratio of 40. The reaction rates of zeolites with a lower Fe content were about half of those of the corresponding aluminum-rich ones. Only [Fe,Al]MFI(0.46,77,st) had an activity nearly equal to its aluminum-rich counterpart [Fe,Al]MFI(0.45,42,st). These materials also exhibited a higher stability, which agrees with the higher benzene and nitrous oxide selectivities. Moreover, we observe a lower contribution of the full combustion route.

The reaction parameters for the calcined counterparts of the isomorphously substituted zeolites with the highest Fe content are also collected in Tables 2 and 3. Clearly, the catalytic performance of the calcined zeolites was lower compared with their steamed counterparts. These catalysts had lower selectivities for phenol, which was mainly due to a larger extent of coke formation.

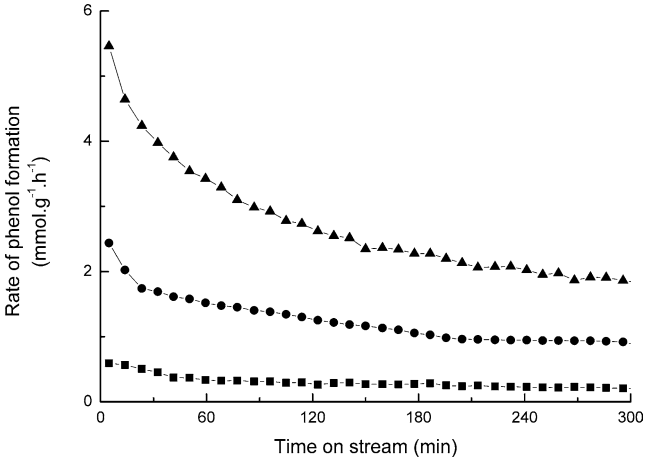

Fig. 3. Rate of phenol formation as a function of reaction time for (■) [Fe,Al]MFI(0.013,78,st), (●) [Fe,Al]MFI(0.089,78,st), and (▲) [Fe,Al]MFI(0.46,77,st) (atmospheric pressure, reaction temperature 623 K, feed composition: 1 vol% benzene, 4 vol% N_2O, 95 vol% He, GHSV 30,000 h^{-1}).

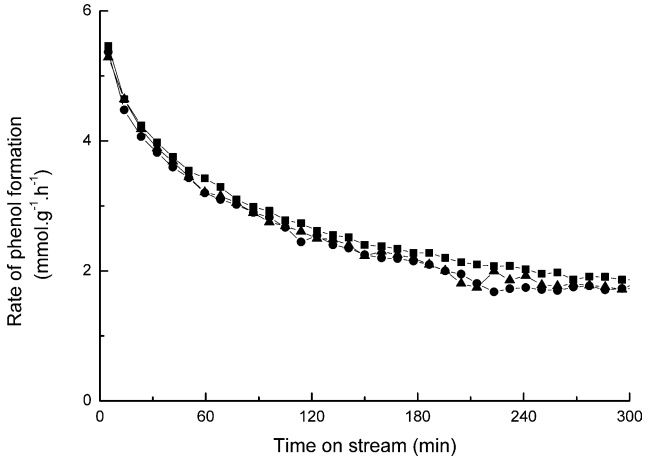

Fig. 4. Rate of phenol formation as a function of reaction time for (■) [Fe,Al]MFI(0.46,77,st), (●) after first regeneration and (▲) after second regeneration (atmospheric pressure, reaction temperature 623 K, feed composition: 1 vol% benzene, 4 vol% N_2O, 95 vol% He, GHSV 30,000 h^{-1}; calcination procedure: from 623 to 823 K at a rate of 2 K min^{-1} in 4 vol% N_2O in He, followed by artificial air calcination at 823 K for 1 h).

To obtain more insight into the regenerability of spent catalysts, we oxidized spent [Fe,Al]MFI(0.46,77,st) and determined the catalytic activity for two consecutive regeneration cycles (Fig. 4). The initial activity could be virtually fully restored by an oxidative treatment, indicating that deactivation was largely due to coke formation.

As outlined earlier [44], [Fe]MFI can be strongly activated for selective benzene oxidation to phenol by the addition of Al. We prepared various zeolites, starting from calcined and steamed [Fe]MFI, by adding Al in the form of trimethylaluminum followed by calcination and steaming treatments. Fig. 5 displays the strong effect of aluminum introduction in [Fe]MFI on the reaction rate. The reaction details are shown in Tables 4 and 5. Calcined (not shown),

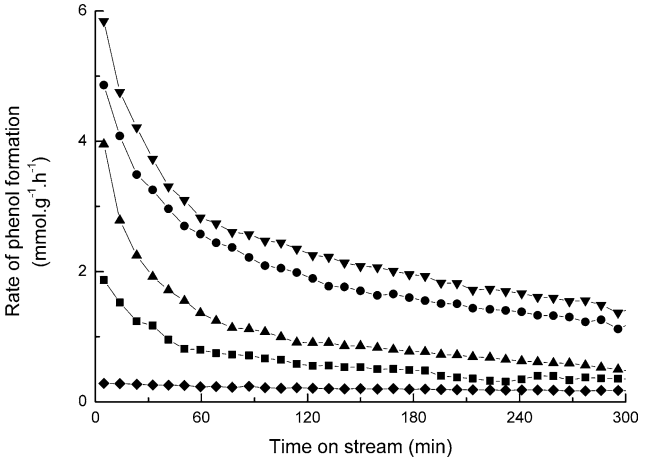

Fig. 5. Rate of phenol formation as a function of reaction time for (◆) [Fe]MFI(st), (■) [Fe]MFI + Me_3Al, (▲) [Fe]MFI + Me_3Al(st), (●) [Fe]MFI(st) + Me_3Al, and (▼) [Fe]MFI(st) + Me_3Al(st) (atmospheric pressure, reaction temperature 623 K, feed composition: 1 vol% benzene, 4 vol% N_2O, 95 vol% He, GHSV 30,000 h^{-1}).

and steamed [Fe]MFI produced only minute amounts of phenol (∼ 0.2 mmol g^{-1} h^{-1}), possibly deriving from the minor amount of Al (approximately 0.005 wt%) contamination. The incorporation of trimethylaluminum followed by calcination significantly increased the rate of formation of the hydroxylated product, mainly by an increase of the selectivity to phenol. For these zeolites the contribution of total combustion was low, initially starting at 1–2% and quickly decreasing within half an hour to less than 1%. This implies an important effect of coke formation as an explanation for the low selectivities. Subsequent steaming further increased the overall performance, mainly by an increase of the benzene conversion. The most active sample was obtained by steaming of [Fe]MFI(st) + Me_3Al(st). These materials generally exhibited lower benzene and nitrous oxide selectivities than steam-activated, isomorphously substituted ones.

A third method for producing active materials is the introduction of Fe into [Al]MFI. This can be achieved by aqueous impregnation of a suitable iron salt (e.g., 10), but this method generally results in iron oxide agglomerates on the external surface. On the other hand, sublimation of $FeCl_3$ has been extensively described [24–26,28–37,39,41–43,45,46] and provides a method for dispersing a molecular Fe species over the protonic sites of the zeolites. Nevertheless, subsequent treatments often lead to a less dispersed and less well-defined iron oxide phase [45]. Fig. 6 presents the reaction rate as a function of the reaction time over various catalysts prepared by sublimation of $FeCl_3$ on iron-free [Al]MFI. The introduction of Fe into [Al]MFI (i.e., [Al]MFI + $FeCl_3$) resulted in phenol formation, in stark contrast to the parent zeolite [Al]MFI. However, the catalyst deactivated quickly, and hardly any activity was observed after approximately 3 h. The reaction parameters in Tables 4 and 5 compare very well with those of Fe/ZSM-5 prepared from a commercial HZSM-5 zeolite [46]. An important difference between this material and those described above is the rela-

Table 4
Initial phenol productivity (R_i), benzene conversion and selectivities to phenol and full combustion products during benzene oxidation for reaction times of 5 min, 1 h and 5 h

Catalyst	R_i [a]	Conversion (%)			Selectivity phenol (%)			Selectivity combustion (%)		
		5 min	1 h	5 h	5 min	1 h	5 h	5 min	1 h	5 h
[Fe]MFI(st)	0.28	9	6	4	12	7	5	<1	<1	<1
[Fe]MFI + Me_3Al	1.87	10	4	1	69	75	>98	2	<1	<1
[Fe]MFI + Me_3Al(st)	4.86	23	9	5	77	>98	>98	2	<1	<1
[Fe]MFI(st) + Me_3Al	3.95	20	5	2	75	90	>98	1	<1	<1
[Fe]MFI(st) + Me_3Al(st)	5.84	25	12	8	90	86	70	<1	<1	<1
[Al]MFI + $FeCl_3$	4.41	31	7	5	53	27	11	10	4	4
[Al]MFI + $FeCl_3$(st)	7.80	42	16	6	70	90	98	6	2	1
[Al]MFI(st) + $FeCl_3$	5.57	32	14	6	65	83	70	6	2	<1
[Al]MFI(st) + $FeCl_3$(st)	8.76	40	18	9	83	94	>98	3	1	<1
Si-1	0.00	0	0	0	0	0	0	–	–	–
Si-1 + Imp(Fe,Al)	0.14	1	<1	<1	50	80	90	<1	<1	<1
Si-1 + Imp(Fe,Al,st)	5.70	23	12	9	94	>98	>98	<1	<1	<1

Note: Reaction temperature 623 K, gas phase composition 1 vol% C_6H_6, 4 vol% N_2O, 95 vol% He, GHSV 30,000 h^{-1}.
[a] Phenol productivity (mmol g^{-1} h^{-1}) after a reaction time of 5 min.

Table 5
Nitrous oxide conversion (X) and selectivity (S) for reaction times of 5 min, 1 h and 5 h

Catalyst	Conversion (%)			Selectivity (%)		
	5 min	1 h	5 h	5 min	1 h	5 h
[Fe]MFI(st)	1	1	1	35	10	2
[Fe]MFI + Me_3Al	3	2	1	53	50	50
[Fe]MFI + Me_3Al(st)	8	2	1	57	>98	>98
[Fe]MFI(st) + Me_3Al	3	2	2	>98	50	20
[Fe]MFI(st) + Me_3Al(st)	4	3	4	>98	>98	40
[Al]MFI + $FeCl_3$	32	12	4	11	4	1
[Al]MFI + $FeCl_3$(st)	25	20	8	30	20	18
[Al]MFI(st) + $FeCl_3$	22	9	7	25	32	16
[A]MFI(st) + $FeCl_3$(st)	19	6	7	44	65	33
Si-1	0	0	0	0	0	0
Si-1 + Imp(Fe,Al)	<1	<1	<1	35	40	60
Si-1 + Imp(Fe,Al,st)	6	3	2	90	>98	>98

Note: Reaction temperature 623 K, gas phase composition 1 vol% C_6H_6, 4 vol% N_2O, 95 vol% He, GHSV 30,000 h^{-1}.

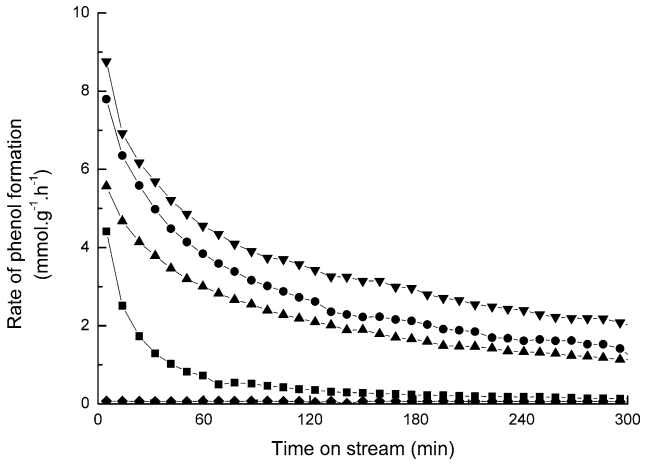

Fig. 6. Rate of phenol formation as a function of reaction time for (◆) [Al]MFI(st), (■) [Al]MFI + $FeCl_3$, (▲) [Al]MFI(st) + $FeCl_3$, (●) [Al]MFI + $FeCl_3$(st), and (▼) [Al]MFI(st) + $FeCl_3$(st) (atmospheric pressure, reaction temperature 623 K, feed composition: 1 vol% benzene, 4 vol% N_2O, 95 vol% He, GHSV 30,000 h^{-1}).

tively high amount of full combustion products formed. For [Al]MFI + $FeCl_3$ this initially amounted to 10%, whereas after 5 h of reaction this route still contributed about 4%. As suggested before [46], cationic or agglomerated iron species might be relevant to this unselective combustion route. These species also show a high nitrous oxide decomposition rate as derived from the high activity of sublimed Fe/ZSM-5 materials [42,43,45,46,50,51] compared with isomorphously substituted ones. We surmise that cationic species are responsible for the direct combustion of benzene. After steam activation, the zeolite had an higher activity and selectivity for phenol. Moreover, the amount of full combustion products substantially decreased. The initial activity, corresponding selectivities, and deactivation behavior were similar to those reported for steam-activated Fe/ZSM-5 [46]. We also found a lower contribution of the combustion route, which was initially 6% and decreased to approximately 1% after 5 h. We explain this by the removal of cationic Fe species decreasing the full combustion pathway. The data also show that the performance improved when the parent [Al]MFI zeolite was steam-activated first, even at a lower Fe content.

Finally, we will further discuss the activities of catalytic materials prepared from a silicalite-1 precursor, which we addressed briefly before [48]. The reaction rate as a function of reaction time is displayed in Fig. 7, and the corresponding reaction data are listed in Tables 4 and 5. The initial substituent-free zeolite (Si-1) expectedly showed no activity in benzene or nitrous oxide conversion. Si-1 + Imp(Fe,st) had an initial rate of phenol formation below 0.02 mmol g^{-1} h^{-1} (not shown). On the other hand, Si-1 + Imp(Fe,Al) displayed a noticeable activity in benzene oxidation with moderate benzene and nitrous oxide selectivities. Although we did not fully characterize these silicalite-1-derived materials, we suggested that after impregnation and calcinations, most of the metal oxide particles will be present on the external surface, most probably in segregated form. However, upon steam treatment the activity increased substantially, and high benzene and nitrous oxide selectivities

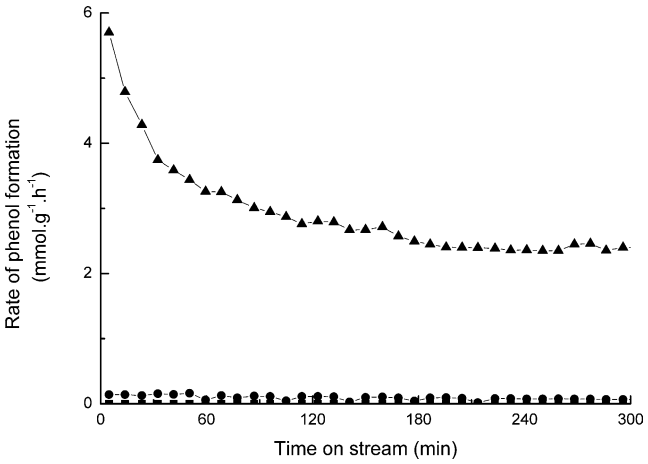

Fig. 7. Rate of phenol formation as a function of reaction time for (■) Si-1, (●) Si-1 + Imp(Fe,Al), and (▲) Si-1 + Imp(Fe,Al,st) (atmospheric pressure, reaction temperature 623 K, feed composition: 1 vol% benzene, 4 vol% N_2O, 95 vol% He, GHSV 30,000 h^{-1}).

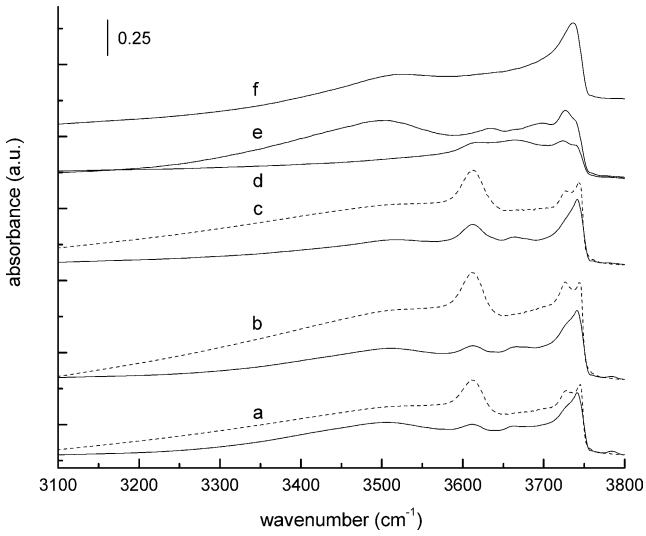

Fig. 8. Room-temperature infrared spectra of the hydroxyl stretching region of the dehydrated zeolites (a) [Fe,Al]MFI(0.015,38), (b) [Fe,Al]MFI(0.092,38), (c) [Fe,Al]MFI(0.45,42), (d) [Fe]MFI + Me_3Al, (e) [Fe]MFI(st) + Me_3Al, and (f) Si-1 + Imp(Fe,Al,st). The spectra of the calcined and steamed zeolites are represented by dotted and full lines, respectively.

were observed. Another point worthy of note is the near-absence of water and carbon dioxide formation for this material. This appears to be in agreement with the absence of cationic exchange sites, where positively charged iron complexes can be accommodated. Although the initial productivity of this material is not the highest reported in the present study, deactivation was minor, and it was the most active catalyst after prolonged reaction times. Thus it may well be that only a relatively small part of the iron and aluminum is dispersed in the zeolite micropore space, resulting in a lower active site density than in the [Fe,Al]MFI catalysts and a lower deactivation rate.

3.2. Infrared spectroscopy

Fig. 8 displays infrared spectra of the hydroxyl stretching region for a limited set of well-dehydrated zeolites. The calcined zeolites with a Si/Al ratio of 40 display similar intensities of the bridging hydroxyl groups. Steam activation resulted in a substantial decrease of the Brønsted acid site density, primarily because of the removal of aluminum from the zeolite framework. On the other hand, we have to take into account that a redistribution of the Fe species to cationic exchange positions may also be relevant to the decrease in the signal of the bridging hydroxyl groups. In addition to these changes, the broad band centered around hydrogen-bonded silanol groups with a maximum around 3500 cm^{-1} sharply decreased in the steamed materials. This is due to further condensation of internal silanol groups [17,48].

The hydroxyl region of [Fe]MFI + Me_3Al indicates the presence of a small number of bridging hydroxyl groups between iron and silicon cations, indicated by the band around 3630 cm^{-1}. This is due to incomplete removal of iron from the framework, even in the presence of Al [52]. Steaming of the starting material ([Fe]MFI(st) instead of [Fe]MFI) before Al introduction resulted in the removal of these framework Fe^{3+} species. Similar to the infrared spectra discussed above, the broad band due to hydrogen-bonded silanol groups decreased sharply. Moreover, a stronger typical hydroxyl band of extraframework AlOH groups was observed for [Fe]MFI(st) + Me_3Al.

The infrared spectrum of the hydroxyl region of Si-1 + Imp(Fe,Al,st) is dominated by isolated silanol groups around 3740 cm^{-1} and a weak broad band around 3500 cm^{-1}. Most importantly, the absence of hydroxyl stretching bands around 3610 and 3630 cm^{-1} indicates that the steaming treatment did not lead to the insertion of noticeable amounts of Fe or Al in the zeolite framework.

Fig. 9 compares the infrared spectra in the region of 1500–1700 cm^{-1} after exposure to NO for 30 min and subsequent evacuation for calcined and steamed zeolites with a Si/Al ratio of 40 with Fe contents in the range of <0.001 to 0.45 wt%. The resulting NO_2 bands are possibly due to a NO_2 impurity in the feed gas, although they may also arise from the interaction of NO with extraframework oxygen atoms. The spectrum of [Al]MFI(st) presents a strong band around 1657 cm^{-1}, which we have argued to be related to NO_2 species coordinating to coordinatively unsaturated extraframework Al species [44]. The shoulder around 1644 cm^{-1} is tentatively assigned to a structural defect of the zeolite, because we also observed this band in calcined [Al]MFI and in [Fe]MFI(st) (not shown). The much higher intensity of the band at 1657 cm^{-1} in steamed [Al]MFI compared with its calcined counterpart agrees well with the extent of dealumination [48]. The spectra for [Fe,Al]MFI(0.0011,39) were expectedly similar to those of [Al]MFI, in view of the very small iron content, and are therefore not shown. The difference between the spectra of calcined [Fe,Al]MFI(0.015,38) and those of calcined [Al]MFI was also minor. However, in the spectra of steamed

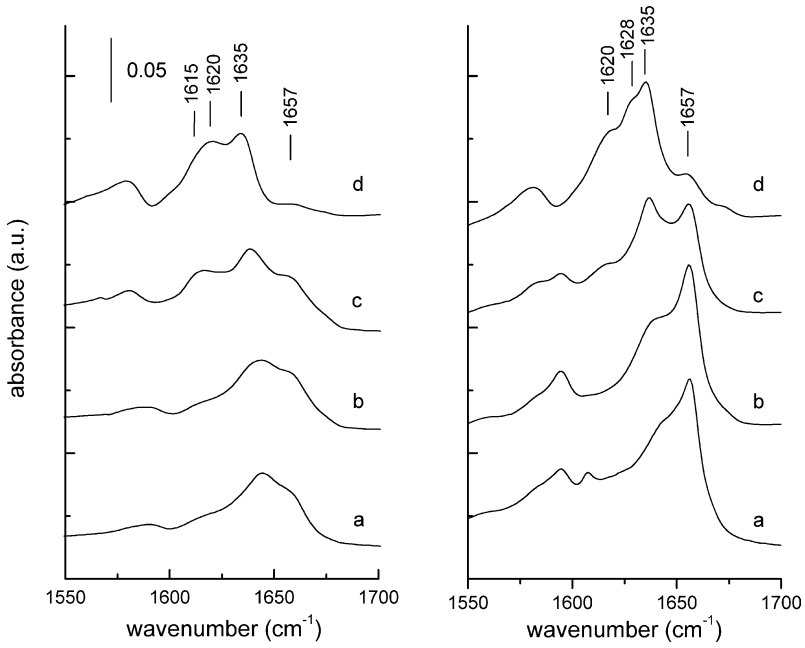

Fig. 9. Infrared spectra of the region 1550–1700 cm^{-1} after exposure to NO and subsequent evacuation for 30 min for (left) calcined and (right) steamed zeolites: (a) [Al]MFI, (b) [Fe,Al]MFI(0.015,38), (c) [Fe,Al]MFI(0.092,38), and (d) [Fe,Al]MFI(0.45,42).

[Fe,Al]MFI(0.015,38) we observe a more pronounced shoulder at 1635 cm^{-1}, which we have attributed to NO_2 species interacting with extraframework Fe–O–Al species [44,48]. This may be due to Fe^{2+} species in Fe–O–Al species.

A further increase of the iron content brought about more pronounced changes in the infrared spectra. For [Fe,Al]MFI (0.092,38), the characteristic feature of NO_2 species in interaction with extraframework Fe around 1615 cm^{-1} was found. Whereas the band at 1657 cm^{-1} did not further increase in calcined [Fe,Al]MFI(0.092,38), this signal was substantially lower in [Fe,Al]MFI(0.092,38,st). Concomitant with this decrease was an increase in the band around 1635 cm^{-1}. The spectra of the zeolites with the highest iron content showed a further decrease of the feature around 1657 cm^{-1}. Simultaneously, the band around 1635 cm^{-1} strongly increased for both calcined and steamed [Fe,Al] MFI(0.45,42).

4. Discussion

4.1. Benzene oxidation with nitrous oxide

Among the isomorphously substituted zeolites, we found that the rate of phenol formation increased with increasing iron and aluminum content. Clearly, steam activation of the calcined precursor increased the initial activity. Generally, the conversions of benzene to phenol after prolonged reaction times were close to quantitative. During the first hour or so, benzene and nitrous oxide selectivities for phenol were lower, and this effect was more pronounced for zeolites with higher Fe and Al content. The contribution of full combustion to this lower selectivity was of minor importance, although this route also became more important at higher substitution levels. The main reason for the lower selectivity lies in the formation of coke products. This is indicated by the possibility of fully restoring the initial activity of [Fe,Al]MFI(0.46,77,st) by calcination.

Coupled with the decrease in benzene conversion with increasing reaction time and increasing Fe content were increases in the selectivities of benzene and nitrous oxide for phenol. This may be explained by a simple consecutive mechanism where benzene is first oxidized to phenol and subsequently to coke products. In the second step nitrous oxide may also be consumed to arrive at dihydroxybenzenes, and acid sites may be involved in condensation reactions. Coke products are thought to consist of dihydroxybenzenes and fused aromatic rings that have been hydroxylated more than once [21,49]. The high boiling points of such compounds impede their desorption from the zeolite micropores and contribute to the inaccessibility of some part of the active sites. Only [Fe,Al]MFI(0.0011,39,st) is relatively stable because of its low activity. Meloni et al. [21] found a relation between the extent of coke formation and the total surface acidity. Our observation that the deactivation due to coking increased with the number of active sites is not necessarily at variance with their conclusion, because the extraframework active species should be Lewis acidic.

These trends were quite different and more difficult to interpret for the catalysts prepared by sublimation of $FeCl_3$ and by the addition of Me_3Al to [Fe]MFI zeolites. In both cases, it is clear that the presence of Fe and Al is essential for selective oxidation of benzene to phenol. However, deactivation of these materials was more pronounced, especially for the calcined precursors. Steaming not only led

to higher activities, but also improved selectivity and stability. We have extensively discussed these effects for sublimed Fe/ZSM-5 before [45,46]. The higher activity upon steaming should be due to extraction of Al from the lattice, resulting in a higher number of active Fe–O–Al species [45]. Nevertheless, we found that steaming also improved the activity of [Al]MFI(st) + $FeCl_3$, which has a lower Fe content than [Al]MFI + $FeCl_3$. This suggests that an additional effect of hydrothermal treatment is the formation of active sites for benzene oxidation. This also holds for the catalysts prepared by the reaction of [Fe]MFI with Me_3Al.

Moreover, a higher initial activity did not always lead to stronger deactivation, as was the case for the isomorphously substituted zeolites. For instance, deactivation for [Al]MFI + $FeCl_3$ was severe, and a steaming pretreatment dramatically improved activity, selectivity, and stability. The extent of full combustion was also highest for [Al]MFI + $FeCl_3$ and decreased upon further steaming. Although not conclusive, we attribute these effects to a strong redistribution of Fe species upon steaming. Cationic species that are abundant in [Al]MFI + $FeCl_3$ are suggested to be important for the full combustion of benzene [46]. Their removal by steaming not only decreased such unwanted side reactions, but also increased the number of sites for selective benzene oxidation [45].

When both Fe and Al were introduced into silicalite-1, we again observed a beneficial effect of hydrothermal treatment. Infrared spectroscopy did not point to insertion of these elements into the zeolite framework, and hence we attribute the improved catalytic performance to the formation of mixed Fe–O–Al species. In fact, this catalyst produced negligible amounts of full combustion products, and its stability was also highest among the catalysts evaluated.

4.2. Nature of the active sites

The catalytic data indicate that iron and aluminum are necessary for selective benzene oxidation to phenol. Inactive [Fe]MFI became active after the addition of (extraframework) Al, and, conversely, [Al]MFI may be activated by the addition of $FeCl_3$. In fact, with proper pre-treatment, the latter method gave the catalyst with the highest initial rate of phenol formation, although the contribution of full combustion is considerable. In general, we observed that steaming treatments improved initial activity and selectivity. This even holds for zeolites to which Fe has been added at extraframework locations. These findings stress the importance of the extraframework location of both Fe and Al and tally with the proposal of an extraframework Fe–O–Al species as an active site for selective benzene oxidation.

For a limited set of catalysts, we have measured NO/NO_2 infrared spectra, which in our belief makes it possible to probe the active sites [47,48]. Fig. 10 shows the relation between the initial rate of phenol formation and the intensity of the band at 1635 cm^{-1} for the series of steamed [Fe,Al]MFI zeolites with Si/Al ratios close to 40, [Fe,Al]MFI(0.089,78,st) and [Fe,Al]MFI(0.45,42). The strong correlation supports our assumption that the band is a signature of the active sites for selective benzene oxidation. Moreover, the proportional increase of the intensity from [Fe,Al]MFI(0.089,78,st) to [Fe,Al]MFI(0.092,38,st) indicates the involvement of Al species in the active site, stressing the role of Al in the active sites [44,46–48]. The correlation is also evident for calcined [Fe,Al]MFI(0.45,42). On the other hand, [Fe]MFI + Me_3Al(st) and [Fe]MFI(st) + Me_3Al(st) exhibited relatively lower activities, as shown in Fig. 10. We tentatively attribute this to diffusion limitations, because of the larger amount of zeolite-occluded extraframework species. This might be due to larger aluminum-containing extraframework species in the micropore space.

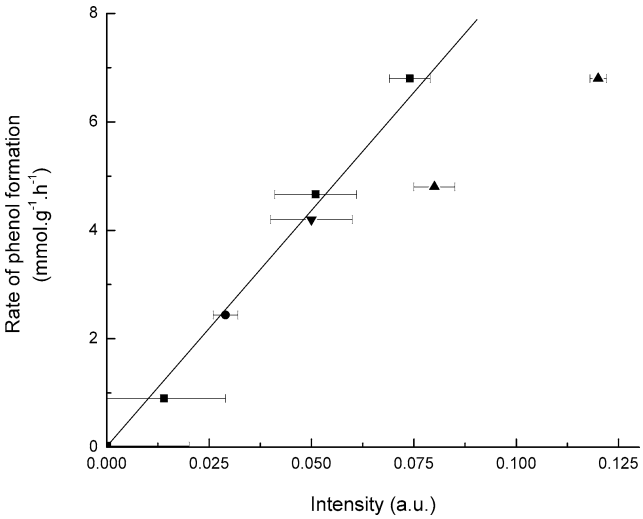

Fig. 10. Relation between initial rate of phenol formation and the intensity of the infrared band at 1635 cm^{-1} for a set of isomorphously substituted [Fe,Al]MFI zeolites with Si/Al ratio close to 40 (■), [Fe,Al]MFI (0.089,78,st) (●), [Fe,Al]MFI(0.45,42) (▼), and two zeolites prepared by exposure of [Fe]MFI to trimethylaluminum (▲).

4.3. Active sites for benzene oxidation and nitrous oxide decomposition

Fig. 11 compares the initial rate of phenol formation at 623 K and nitrous oxide decomposition rate at 760 K as a function of the iron content for the steam-activated, isomorphously substituted zeolites with Si/Al close to 40. Clearly, the rate of the hydroxylation reaction increased strongly at very low Fe contents and leveled off at higher Fe loadings. Assuming that all Fe atoms in [Fe,Al]MFI(0.0011,39,st) are incorporated into sites for benzene oxidation, the linear increase in activity up to an Fe content of 0.092 wt% suggests that 0.018 wt% Fe took part in the selective oxidation reaction in [Fe,Al]MFI(0.092,38,st). This amounts to approximately 2×10^{18} sites g^{-1} and is well within the range of active site densities determined for similar catalysts prepared by Dubkov et al. [10]. Note that this also implies that only very small amounts of (extraframework) Al are involved in the selective oxidation reaction.

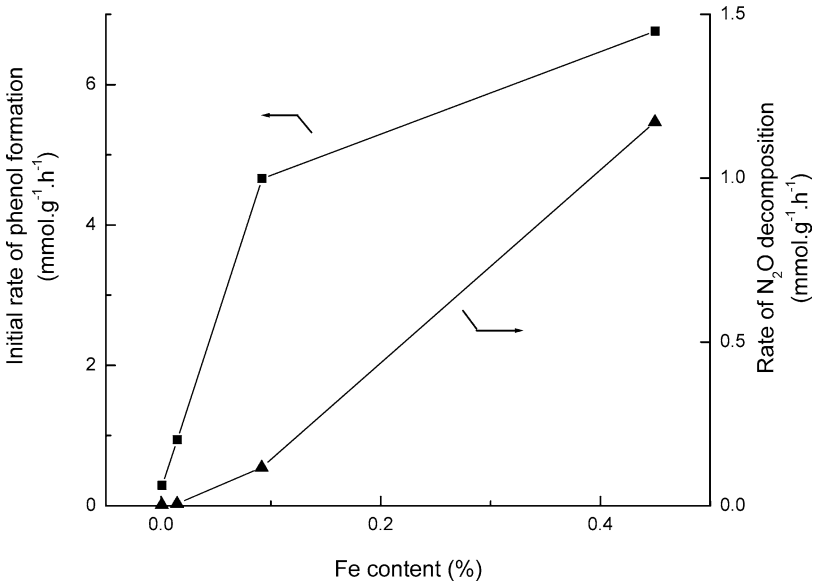

Fig. 11. Initial rate of phenol formation (■) during benzene oxidation and nitrous oxide reaction rate at 760 K (▲) during its decomposition as a function of the iron content for a set of steam-activated isomorphously substituted [Fe,Al]MFI zeolites with Si/Al ratio close to 40.

On the other hand, the nitrous oxide decomposition rate at 760 K for the same set of catalysts was relatively low for low iron contents but strongly increased at higher iron contents. These very deviant trends for benzene oxidation and nitrous oxide decomposition suggest that the active sites for the two reactions are different. At the reaction temperature for benzene oxidation (623 K), the nitrous oxide conversion was negligible for all catalysts. This implies that removal of deposited oxygen atoms is due mainly to benzene and the hydroxylated product molecules and not to reduction by nitrous oxide or molecular oxygen recombination.

Although it is most likely that the sites for selective oxidation become catalytically active in nitrous oxide decomposition at higher temperatures, their low abundance and the high nitrous oxide decomposition rate at elevated temperatures imply unrealistically high turnover numbers. It is thus more likely that nitrous oxide decomposition also takes place over other Fe-containing species. Further support is provided by the trend in Fig. 11 for nitrous oxide decomposition. The disproportional increase indicates that a certain degree of Fe agglomeration is necessary for good performance in nitrous oxide decomposition at higher temperatures. This agrees well with the view of Pérez-Ramírez et al. [52–54]. One should thus distinguish between a very minor fraction of Fe sites active in benzene oxidation at low temperature, which may be titrated by *low-temperature* nitrous oxide decomposition, and a larger fraction of more clustered Fe species that contribute to nitrous oxide decomposition at more elevated temperatures.

5. Conclusions

A study of the benzene oxidation activity of a suite of MFI-type zeolites prepared via various routes further substantiates the assignment of the active sites to an extraframework mixed Fe and Al oxide species. Active materials for phenol production may be prepared via extraction of Fe and Al from framework locations after isomorphous substitution during zeolite synthesis, the use of molecular Fe and Al precursors over alumino- and ferrosilicalites, and the post-synthesis dispersion of Fe and Al in siliceous MFI zeolite. Further conclusions are as follows:

- The most active and selective materials are prepared by steam activation of isomorphously substituted Fe- and Al-containing zeolites. A high initial activity is coupled with strong deactivation due to coke formation. This leads to a decrease in the catalytic surface, a decrease in the benzene conversion, and an increase in the selectivity for phenol.
- Hydrothermal treatment at elevated temperatures appears to have two effects: (i) the removal of heteroatoms from the MFI framework and (ii) promotion of the formation of mixed Fe–O–Al species, which is possibly due to an increased mobility of oxide species.
- The rate of phenol formation increased with increasing Fe and Al content for steam-activated, isomorphously substituted zeolites. The amount of Fe incorporated into the active sites for selective benzene oxidation was only minor and was estimated to be in the range of 10^{18} to 10^{19} g^{-1}. However, other, more clustered Fe-containing species appear to be important to nitrous oxide decomposition at higher temperatures.
- Active materials show an infrared band at 1635 cm^{-1} after exposure to NO (NO_2). This band is surmised to be related to NO_2 coordinating to Fe–O–Al species. The positive correlation between its intensity and the initial

rate of phenol formation suggests that this infrared band is a signature of the active sites.

Despite these similarities, some important differences are noted in the performance of the various materials:

- The degree of full combustion decreased in the order of zeolites prepared by sublimation of $FeCl_3$ to [Al]MFI > steam-activated isomorphously substituted zeolites > trimethylaluminum-loaded [Fe]MFI > iron- and aluminium-impregnated silicalite-1. The combustion appears to be due to cationic Fe species that are able to activate nitrous oxide and oxidize benzene or phenol.
- Catalysts prepared by grafting of molecular species exhibited rates of phenol formation similar to those of hydrothermally synthesized catalysts but generally had somewhat lower benzene and nitrous oxide selectivities. However, steaming of silicalite-1 impregnated with iron and aluminum nitrate rendered a catalyst with high selectivities and a rather low deactivation rate.

References

[1] G. Centi, F. Cavani, F. Trifirò, Selective Oxidation by Heterogeneous Catalysis, Kluwer Academic, New York, 2001.
[2] V.L. Zholobenko, I.N. Senchenya, L.M. Kustov, V.B. Kazansky, Kinet. Catal. 32 (1991) 151.
[3] R. Burch, C. Howitt, Appl. Catal. A 103 (1993) 135.
[4] J.L. Motz, H. Heinrichen, W.F. Hölderich, J. Mol. Catal. A 136 (1998) 175.
[5] G.I. Panov, V.I. Sobolev, A.S. Kharitonov, J. Mol. Catal. 61 (1990) 85.
[6] A.S. Kharitonov, G.A. Sheveleva, G.I. Panov, V.I. Sobolev, Y.A. Paukshtis, V.N. Romannikov, Appl. Catal. 98 (1993) 33.
[7] G.I. Panov, V.I. Sobolev, K.A. Dubkov, V.N. Parmon, N.S. Ovanesyan, A.E. Shilov, A.A. Shteinman, React. Kinet. Catal. Lett. 61 (1997) 251.
[8] P. Notté, Top. Catal. 13 (2000) 387.
[9] L.V. Pirutko, V.S. Chernyavsky, A.K. Uriarte, G.I. Panov, Appl. Catal. A 227 (2002) 143.
[10] K.A. Dubkov, N.S. Ovanesyan, A.A. Shteinman, E.V. Starokon, G.I. Panov, J. Catal. 207 (2002) 341.
[11] P. Ratnasamy, R. Kumar, Catal. Today 9 (1991) 329.
[12] A. Ribera, I.W.C.E. Arends, S. de Vries, J. Pérez-Ramírez, R.A. Sheldon, J. Catal. 195 (2000) 287.
[13] J. Pérez-Ramírez, F. Kapteijn, G. Mul, X. Xu, J.A. Moulijn, Catal. Today 76 (2002) 55.
[14] G. Mul, J. Pérez-Ramírez, F. Kapteijn, J.A. Moulijn, Catal. Lett. 80 (2002) 129.
[15] J. Pérez-Ramírez, G. Mul, F. Kapteijn, J.A. Moulijn, A.R. Overweg, A. Doménech, A. Ribera, I.W.C.E. Arends, J. Catal. 207 (2002) 113.
[16] J. Pérez-Ramírez, F. Kapteijn, K. Schöffel, J.A. Moulijn, Appl. Catal. B 44 (2003) 117.
[17] S. Bordiga, R. Buzzoni, F. Geobaldo, C. Lamberti, E. Giamello, A. Zecchina, G. Leofanti, G. Petrini, G. Tozzola, G. Vlaic, J. Catal. 158 (1996) 486.
[18] G. Berlier, G. Spoto, S. Bordiga, G. Ricchiardi, P. Fisicaro, A. Zecchina, I. Rossetti, E. Selli, L. Forni, E. Giamello, C. Lamberti, J. Catal. 208 (2002) 64.
[19] A.M. Ferretti, C. Oliva, L. Forni, G. Berlier, A. Zecchina, C. Lamberti, J. Catal. 208 (2002) 83.
[20] G. Berlier, A. Zecchina, G. Spoto, G. Ricchiardi, S. Bordiga, C. Lamberti, J. Catal. 215 (2003) 264.
[21] D. Meloni, R. Monaci, V. Solinas, G. Berlier, S. Bordiga, I. Rossetti, C. Oliva, L. Forni, J. Catal. 214 (2003) 169.
[22] G. Berlier, A. Zecchina, G. Spoto, G. Ricchiardi, S. Bordiga, C. Lamberti, J. Catal. 213 (2003) 264.
[23] G. Centi, C. Genovese, G. Giordano, A. Katovic, S. Perathoner, Catal. Today 91–92 (2004) 17.
[24] P. Marturano, A. Kogelbauer, R. Prins, J. Catal. 190 (2000) 460.
[25] P. Marturano, L. Drozdová, A. Kogelbauer, R. Prins, J. Catal. 192 (2000) 236.
[26] G.D. Pirngruber, M. Luechinger, P.K. Roy, A. Cecchetto, P. Smirniotis, J. Catal. 224 (2004) 429.
[27] L.J. Lobree, I.-C. Hwang, J.A. Reimer, A.T. Bell, Catal. Lett. 63 (1999) 233.
[28] H.-Y. Chen, W.M.H. Sachtler, Catal. Lett. 50 (1998) 125.
[29] H.-Y. Chen, T. Voskobonikov, W.M.H. Sachtler, J. Catal. 180 (1998) 171.
[30] H.-Y. Chen, T. Voskoboinikov, W.M.H. Sachtler, Catal. Today 54 (1999) 483.
[31] H.-Y. Chen, El-M. El-Malki, X. Wang, R.A. van Santen, W.M.H. Sachtler, J. Mol. Catal. 162 (2000) 159.
[32] H.-Y. Chen, X. Wang, W.M.H. Sachtler, Phys. Chem. Chem. Phys. 2 (2000) 3083.
[33] El-M. El-Malki, R.A. van Santen, W.M.H. Sachtler, Micropor. Mesopor. Mater. 35–36 (2000) 235.
[34] El-M. El-Malki, R.A. van Santen, W.M.H. Sachtler, J. Catal. 196 (2000) 212.
[35] J. Jia, B. Wen, W.M.H. Sachtler, J. Catal. 210 (2002) 453.
[36] J. Jia, K.S. Pillai, W.M.H. Sachtler, J. Catal. 221 (2004) 119.
[37] F. Heinrich, C. Schmidt, E. Löffler, M. Menzel, W. Grünert, J. Catal. 212 (2002) 157.
[38] P. Kubánek, B. Wichterlová, Z. Sobalík, J. Catal. 211 (2002) 109.
[39] A.A. Battiston, J.H. Bitter, F.M.F. de Groot, A.R. Overweg, O. Stephan, J.A. van Bokhoven, P.J. Kooyman, C. van der Spek, G. Vankó, D.C. Koningsberger, J. Catal. 213 (2003) 251.
[40] P. Fejes, I. Kiricsi, K. Lázár, I. Marsi, A. Rockenbauer, L. Korecz, J.B. Nagy, R. Aiello, F. Testa, Appl. Catal. A 242 (2003) 247.
[41] I. Yuranov, D.A. Bulushev, A. Renken, L. Kiwi-Minsker, J. Catal. 227 (2004) 138.
[42] Q. Zhu, E.J.M. Hensen, B.L. Mojet, J.H.M.C. van Wolput, R.A. van Santen, Chem. Commun. (2002) 1232.
[43] Q. Zhu, B.L. Mojet, R.A.J. Janssen, E.J.M. Hensen, J. van Grondelle, P.C.M.M. Magusin, R.A. van Santen, Catal. Lett. 81 (2002) 205.
[44] E.J.M. Hensen, Q. Zhu, R.A. van Santen, J. Catal. 220 (2003) 260.
[45] E.J.M. Hensen, Q. Zhu, M.M.R.M. Hendrix, A.R. Overweg, P.J. Kooyman, M.V. Sychev, R.A. van Santen, J. Catal. 221 (2004) 560.
[46] Q. Zhu, R.M. van Teeffelen, R.A. van Santen, E.J.M. Hensen, J. Catal. 221 (2004) 575.
[47] E.J.M. Hensen, Q. Zhu, P.-H. Liu, K.-J. Chao, R.A. van Santen, J. Catal. 226 (2004) 466.
[48] E.J.M. Hensen, Q. Zhu, R.A.J. Janssen, P.C.M.M. Magusin, P.J. Kooyman, R.A. van Santen, J. Catal. 233 (2005) 123.
[49] A.A. Ivanov, V.S. Chernyavsky, M.J. Gross, A.S. Kharitonov, A.K. Uriarte, G.I. Panov, Appl. Catal. A 249 (2003) 327.
[50] G.D. Pirngruber, J. Catal. 219 (2003) 456.
[51] P.K. Roy, G.D. Pirngruber, J. Catal. 227 (2004) 164.
[52] J. Pérez-Ramírez, J. Catal. 227 (2004) 512.
[53] J. Pérez-Ramírez, F. Kapteijn, G. Mul, J.A. Moulijn, Catal. Commun. 3 (2002) 19.
[54] J. Pérez-Ramírez, F. Kapteijn, A. Brückner, J. Catal. 218 (2002) 234.